

Mechanisms of Discordant Alternans and Induction of Reentry in Simulated Cardiac Tissue

Zhilin Qu, PhD; Alan Garfinkel, PhD; Peng-Sheng Chen, MD; James N. Weiss, MD

Background—T-wave alternans, which is associated with the genesis of cardiac fibrillation, has recently been related to discordant action potential duration (APD) alternans. However, the cellular electrophysiological mechanisms responsible for discordant alternans are poorly understood.

Methods and Results—We simulated a 2D sheet of cardiac tissue using phase 1 of the Luo-Rudy cardiac action potential model. A steep (slope >1) APD restitution curve promoted concordant APD alternans and T-wave alternans without QRS alternans. When pacing was from a single site, discordant APD alternans occurred only when the pacing rate was fast enough to engage conduction velocity (CV) restitution, producing both QRS and T-wave alternans. Tissue heterogeneity was not required for this effect. Discordant alternans markedly increases dispersion of refractoriness and increases the ability of a premature stimulus to cause localized wavebreak and induce reentry. In the absence of steep APD restitution and of CV restitution, sustained discordant alternans did not occur, but reentry could be induced if there was marked electrophysiological heterogeneity. Both discordant APD alternans and preexisting APD heterogeneity facilitate reentry by causing the waveback to propagate slowly.

Conclusion—Discordant alternans arises dynamically from APD and CV restitution properties and markedly increases dispersion of refractoriness. Preexisting and dynamically induced (via restitution) dispersion of refractoriness independently increase vulnerability to reentrant arrhythmias. Reduction of dynamically induced dispersion by appropriate alteration of electrical restitution has promise as an antiarrhythmic strategy. (*Circulation*. 2000;102:1664-1670.)

Key Words: alternans ■ arrhythmias ■ reentry ■ action potentials

T-wave alternans is closely associated with the vulnerability to ventricular arrhythmias and sudden cardiac death.¹⁻⁵ The transition from concordant to discordant action potential duration (APD) alternans is also a harbinger of vulnerability to ventricular fibrillation.⁶⁻¹⁰ Recent optical mapping studies by Pastore et al⁹ linked these 2 findings by demonstrating that with increasing pacing rate, APD first alternates concordantly throughout the tissue (causing T-wave alternans) and then becomes spatially discordant, with areas of long-short APD alternation adjacent to areas with short-long APD alternation (causing both QRS and T-wave alternans). This spatially out-of-phase APD alternation reflects a state of markedly increased dispersion of refractoriness, which predisposes the heart to wavebreak and initiation of reentry. Despite the importance of APD alternans as the basis for T-wave alternans, however, “the mechanisms responsible for initiating discordant alternans are unknown.”⁹ It has been shown that for APD alternans to occur, an APD restitution slope >1 is required.¹¹⁻¹⁴ We hypothesize that in addition to steep APD restitution, the engagement of conduc-

tion velocity (CV) restitution is required for the transition from concordant alternans to discordant alternans to occur. In this study, we simulated 2D cardiac tissue to investigate the cellular electrophysiological basis for discordant alternans, particularly the roles of electrical restitution and tissue heterogeneity. We also examined the mechanism by which rapid pacing and premature stimuli induce reentry and ventricular fibrillation in the setting of discordant alternans and tissue heterogeneity.

Methods

We simulated a monodomain 2D sheet (with “no-flux” boundary conditions) of cardiac tissue¹⁵ using the equation

$$(1) \quad C_m \frac{\partial V}{\partial t} = -I_{ion} + \frac{1}{\rho_x S_v} \frac{\partial^2 V}{\partial x^2} + \frac{1}{\rho_y S_v} \frac{\partial^2 V}{\partial y^2},$$

where $C_m = 1 \mu\text{F}/\text{cm}^2$ is transmembrane capacitance, V is transmembrane voltage, $\rho_x = \rho_y = 0.5 \text{ k}\Omega \text{ cm}$ are gap junction resistivity, and $S_v = 2000 \text{ cm}^{-1}$ is the surface-to-volume ratio. I_{ion} , the current density, was generated by phase 1 of the Luo-Rudy (LR1) action potential model.¹⁶ The LR1 model was modified to achieve desired APD and

Received February 15, 2000; revision received May 2, 2000; accepted May 8, 2000.

From the Cardiovascular Research Laboratory and the Departments of Medicine (Cardiology), Physiology, and Physiological Science, UCLA, and Cedars-Sinai Medical Center, Los Angeles, Calif.

Correspondence to Zhilin Qu, PhD, Cardiovascular Research Laboratory, MRL 3645, UCLA School of Medicine, 675 Charles E. Young Dr South, Los Angeles, CA 90095-1760. E-mail zqu@ucla.edu

© 2000 American Heart Association, Inc.

Circulation is available at <http://www.circulationaha.org>

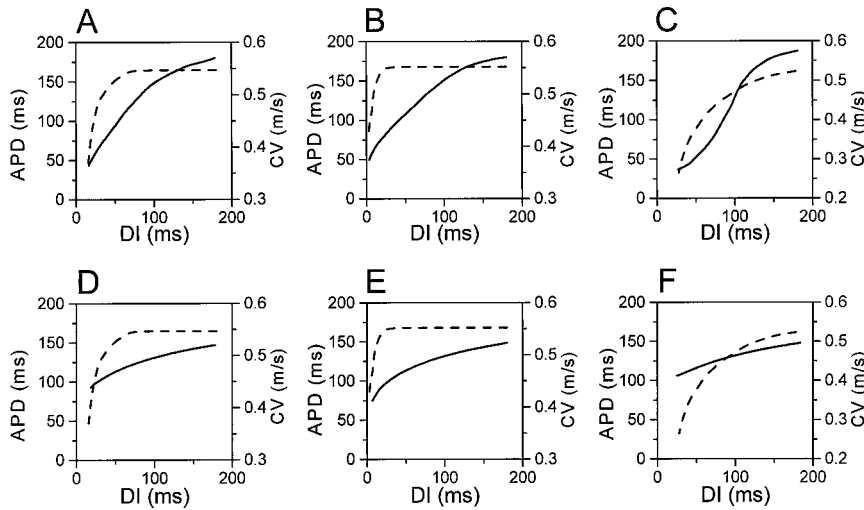


Figure 1. Combinations of APD (solid lines) and CV (dashed lines) restitution. A through C, Steep APD restitution, with normal (A), narrowed (B), or broadened (C) CV restitution. D through F, Shallow APD restitution with corresponding alterations in CV restitution. Parameter changes from LR1 model are $\bar{G}_{Na}=16$ mS/cm², $\bar{G}_K=0.423$ mS/cm²; A, $\bar{G}_{Si}=0.055$ mS/cm²; B, $\bar{G}_{Si}=0.055$ mS/cm²; $j=1$ (j gate was clamped); C, $\bar{G}_{Si}=0.055$ mS/cm², $\tau_j \rightarrow 5\tau_j$; D, $\bar{G}_{Si}=0.09$ mS/cm², $\tau_d \rightarrow 0.3\tau_d$, $\tau_f \rightarrow 0.3\tau_f$; E, $\bar{G}_{Si}=0.09$ mS/cm², $\tau_d \rightarrow 0.3\tau_d$, $\tau_f \rightarrow 0.3\tau_f$, $j=1$; F, $\bar{G}_{Si}=0.09$ mS/cm², $\tau_d \rightarrow 0.3\tau_d$, $\tau_f \rightarrow 0.3\tau_f$, $j=1$.

CV restitution properties, as stated in Figure 1; unless otherwise stated, parameter values are the same as the original LR1 model (we set $[K]_0=5.4$ mmol/L). We integrated Equation 1 using our advanced method¹⁷ with time step varying adaptively from 0.01 to 0.2 ms and fixed 0.015-cm space step.

Electrophysiological heterogeneity was modeled by changing K^+ channel conductance as follows:

$$(2) \quad \bar{G}_K(x,y) = \bar{G}_K \{ \alpha + \beta \sqrt{[(x-L_x)^2 + (y-L_y)^2] / (L_x^2 + L_y^2)} \},$$

where x and y are the tissue coordinates, L_x and L_y are the dimensions of the tissue, $\bar{G}_K=0.282$ mS/cm², $\alpha=1.2$, and $\beta=0.8$. This produced an electrophysiological heterogeneity similar to that observed in guinea pig ventricle.¹⁸ Equation 2 was modified to vary the degree of heterogeneity as specified.

Pacing stimuli (S_1) and premature stimuli (S_2) were delivered to a 0.15×0.15 -cm area at the lower left corner ($x=y=0$) with a strength of $30 \mu A/cm^2$ (≈ 1.5 times threshold), unless otherwise specified. APD and diastolic interval (DI) were defined as the durations that $V > -72$ mV and $V < -72$ mV, respectively. APD dispersion was calculated as

$$(3) \quad \sigma = \sqrt{\frac{1}{N} \sum_{i=1}^N (APD_i - \langle APD \rangle)^2},$$

where N is the total number of grid points we used in the simulation and $\langle APD \rangle$ is the spatially averaged APD.

Results

Electrical Restitution

To study APD and CV restitution effects, we modified LR1 kinetics to produce 2 types of APD restitution and 3 different types of CV restitution, for a total of 6 combinations. One APD restitution type had slope >1 over a wide range of DIs (Figure 1, A through C), and the other had slope <1 everywhere (Figure 1, D through F). CV restitution types differed in the range of DIs over which CV varied: either the normal range for the LR1 model (Figure 1, A and D), a shortened range (Figure 1, B and E), or a broadened range (Figure 1, C and F). Details of the parameter changes are stated in the Figure 1 legend.

Modulation of Dispersion by Premature Stimulus

In intact guinea pig ventricle, Laurita et al¹⁸ found that dispersion of APD during a premature stimulus decreased to

a minimum before progressively increasing as the coupling interval was shortened. To investigate the roles of electrical restitution and electrophysiological heterogeneity, we compared electrophysiologically homogeneous and heterogeneous tissue by use of various APD and CV restitution combinations shown in Figure 1.

Homogeneous Tissue

For homogeneous tissue, the dispersion of APD (σ) was almost zero for long S_1S_2 coupling intervals, increasing monotonically as the coupling interval decreased (Figure 2A). There was no dip in σ before the increase, because σ was

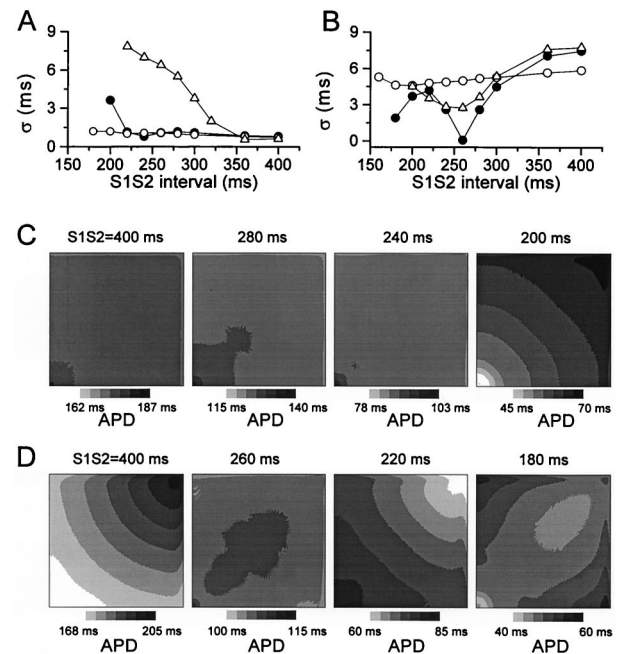


Figure 2. APD dispersion (σ) versus S_1S_2 coupling interval. A, Homogeneous tissue with steep APD restitution and either normal (\bullet), narrowed (\circ), or broadened CV restitution (\triangle). B, Heterogeneous tissue with steep APD restitution and either normal (\bullet) or broadened (\triangle) CV restitution and with shallow APD restitution and normal CV restitution (\circ). C and D, Spatial APD distributions in homogeneous (C) and heterogeneous (D) tissue at different S_1S_2 coupling intervals for steep APD restitution plus normal CV restitution (as in Figure 1A).

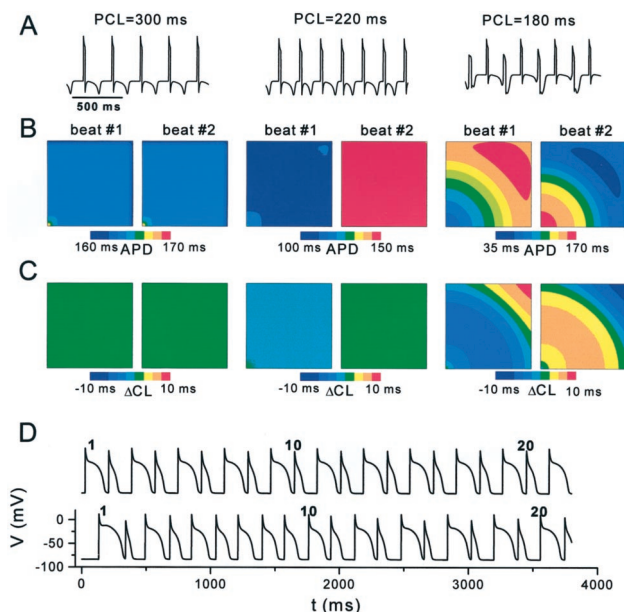


Figure 3. Transition from concordant (middle panels) to discordant (right panels) alternans in homogeneous tissue during constant pacing for steep APD restitution plus normal CV restitution (as in Figure 1A). A, Pseudo-ECG illustrating no alternans (PCL=300 ms), T-wave alternans (PCL=220 ms), and QRS plus T-wave alternans (PCL=180 ms). B and C, Spatial APD distribution (B) and ΔCL (=CL-PCL) distribution (C) for 2 successive beats at different PCLs. D, Membrane voltage records from 2 different sites in tissue, showing discordant alternans. 1, 10, and 20 mark corresponding beats at each site.

already near zero. The S_1S_2 coupling interval at which σ increased was determined by CV restitution. Broadening the range of DIs over which CV changed caused σ to increase at longer S_1S_2 coupling intervals (Δ), and narrowing the range had the opposite effect (\circ). Figure 2C shows the spatial distribution of APD in homogeneous tissue with steep APD restitution plus normal CV restitution (corresponding to Figure 1A) during baseline pacing and during a premature stimulus at 3 different S_1S_2 coupling intervals.

Heterogeneous Tissue

For electrophysiologically heterogeneous tissue, σ was non-zero (by construction) during baseline pacing. For steep APD restitution plus normal CV restitution (corresponding to Figure 1A), σ decreased to a minimum and then increased as the S_1S_2 coupling interval was shortened (Figure 2B, \bullet), similar to intact guinea pig ventricle (Figures 5 and 8B in Laurita et al¹⁸ and Figure 4A in Laurita et al¹⁹). Figure 2D shows corresponding spatial maps of APD during baseline pacing and premature stimuli at 3 different S_1S_2 coupling intervals. Altering CV restitution affected the range of S_1S_2 coupling intervals over which the dip occurred (eg, Δ in Figure 2B, corresponding to steep APD restitution plus broadened CV restitution in Figure 1C), but the dip remained prominent. In contrast, flattening APD restitution (corresponding to Figure 1, D through F) markedly attenuated the dip, with σ remaining nearly constant irrespective of CV restitution properties (Figure 2B, \circ).

Transition From Concordant Alternans to Discordant Alternans

To study how concordant and discordant APD alternans develop, we rapidly paced homogeneous or heterogeneous 2D tissue with different APD and CV restitution characteristics.

Homogeneous Tissue

Figure 3 shows the pseudo-ECG, APD alternans, and CL alternans at different pacing cycle lengths (PCLs) in homogeneous tissue. At PCL=300 ms, there was no alternans. At PCL=220 ms, concordant APD alternans developed, but no CL alternans. At PCL=180 ms, CL alternans began and APD alternans became discordant. During concordant alternans, the pseudo-ECG showed only T-wave alternans, without QRS alternans. With discordant alternans, both the T-wave and the QRS complex alternated. This result is very similar to the findings of Pastore et al⁹ (their Figures 4 and 6). Thus, preexisting electrophysiological heterogeneity is not required for concordant or discordant alternans or for QRS or T-wave alternans.

Figure 4, A through C summarizes the maximum differences in APD (\bullet) and CL (\circ) versus PCL in homogeneous tissue with steep APD restitution and different CV restitution properties (corresponding to Figure 1, A through C, respectively). With normal CV restitution (Figure 4A), CL alternans occurred after APD alternans. With CV restitution narrowed (Figure 4B), APD alternans occurred, but CL alternans never developed. With CV restitution broadened (Figure 4C), APD alternans and CL alternans occurred simultaneously. CL alternans was invariably associated with the onset of discordant APD alternans. For flat APD restitution (corresponding to Figure 1, D through F), neither APD nor CL alternans was

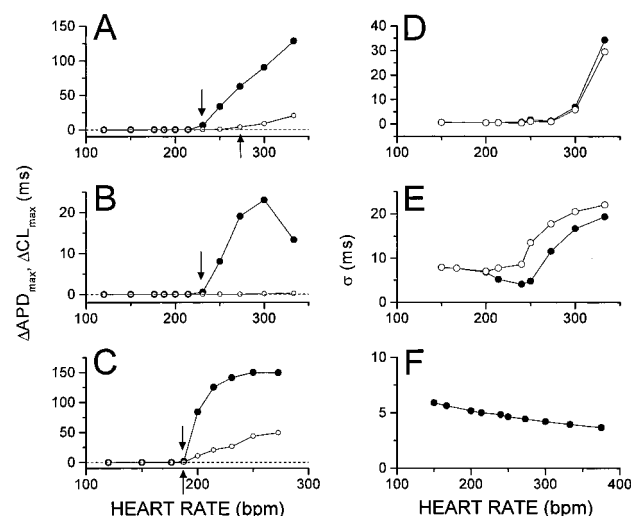


Figure 4. A through C, Maximum differences in APD (\bullet) and CL (\circ) in homogeneous tissue versus heart rate with steep APD restitution and either normal (A), narrowed (B), or broadened (C) CV restitution. Downward and upward arrows indicate onset of concordant and discordant alternans, respectively. D through F, APD dispersion (σ) of 2 successive beats (\circ and \bullet) vs heart rate. D and E, Homogeneous (D) and heterogeneous (E) tissue, with steep APD restitution plus normal CV restitution (as in Figure 1A), respectively. F, Heterogeneous tissue, with shallow APD restitution plus normal CV restitution (as in Figure 1D).

observed at any PCL, although a mild dispersion of APD was present, similar to Figure 3B.

Heterogeneous Tissue

Figure 4, D through F compares the dispersion of APD during 2 successive beats as a function of PCL in homogeneous (Figure 4D) and electrophysiologically heterogeneous (Figure 4, E and F) tissues. The result in Figure 4E, with steep APD restitution and normal CV restitution, is similar to the results of Pastore et al⁹ in guinea pig ventricle (their Figure 7). When APD restitution is shallow (corresponding to Figure 1D), σ decreased slightly with decreasing PCL and never increased even at the shortest PCL with 1:1 conduction (Figure 4F), consistent with the failure of discordant APD alternans to develop. The detailed mechanism underlying discordant alternans is presented in the Appendix.

Discordant Alternans and the Induction of Reentry

To explore the relationship between electrical alternans and reentry, homogeneous and heterogeneous tissues were paced from the lower left corner for 15 beats at a fixed PCL (S_1), followed by a premature stimulus (S_2) to induce reentry.

Homogeneous Tissue

In homogeneous tissue, an S_2 stimulus delivered at the S_1 site did not induce reentry. To induce reentry, S_2 had to be delivered at a different site from S_1 to break symmetry. Accordingly, S_2 was applied along the diagonal from the lower left to the upper right corners. Figure 5, A and B, summarizes the vulnerable window for induction of reentry versus distance of S_2 along the diagonal. At long PCLs without APD alternans (Figure 5A), the S_2 either propagated or failed but never induced reentry. Only when the PCL was short enough to induce discordant alternans could reentry be induced by an S_2 in a proper position (Figure 5B). Thus, induction of reentry by a premature stimulus during discordant alternans did not require preexisting electrophysiological heterogeneity if S_2 was delivered at a different site from S_1 .

Heterogeneous Tissue

In heterogeneous tissue, an S_2 delivered at the S_1 site could induce reentry, because symmetry was broken by the preexisting tissue heterogeneity. Figure 6 illustrates reentry induction by an S_2 , which is similar to the example shown in guinea pig heart⁹ (see their Figure 8). Conduction block occurred at a location where APDs were in their long phase during discordant alternans (Figure 6B, middle). This local conduction block resulted in figure-eight reentry (fourth panel) and subsequent breakup into a fibrillation-like state (fifth panel).

Induction of reentry by this protocol depended on both electrical restitution properties and the degree of preexisting electrophysiological heterogeneity, in addition to the S_1 and S_1S_2 intervals. Figure 5, C through F, summarizes the phase diagrams for several restitution combinations. For steep APD restitution plus normal CV restitution (as in Figure 1A), there was a large vulnerable window for S_2 to induce reentry at short PCLs, which narrowed and disappeared as the PCL increased (Figure 5C), similar to homogeneous tissue. If the degree of preexisting electrophysiological heterogeneity was

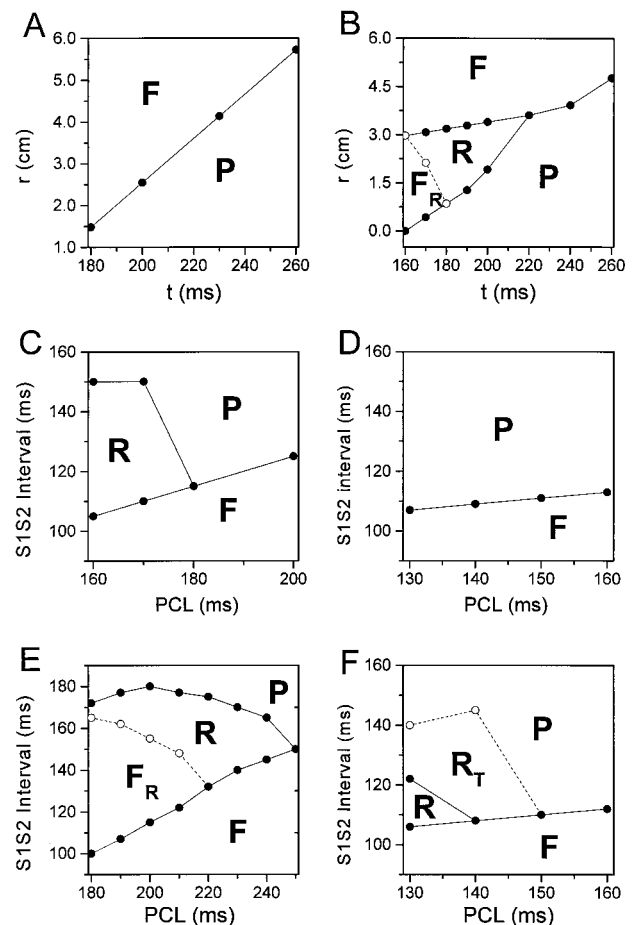


Figure 5. A and B, Phase diagram in space-time for vulnerability to reentry by a premature stimulus (S_2) in homogeneous tissue with steep APD restitution plus normal CV restitution (as in Figure 1A) at 2 PCLs: 300 ms (A) and 180 ms (B). Fifteen S_1 beats were delivered to lower left corner of tissue. S_2 was delivered at time t after the last S_1 stimulus at distance r along diagonal line from lower left to upper right corners. C through F, Phase diagram for vulnerability to reentry by a premature stimulus (S_2) as a function of S_1 PCL in heterogeneous tissue under the following conditions: for C, steep APD restitution plus normal CV restitution (as in Figure 1A); for D, shallow APD restitution plus normal CV restitution (as in Figure 1D); for E, as in A, except with decreased heterogeneity ($\beta=0.4$ in Equation 2); for F, as in B, except with increased tissue heterogeneity (in Equation 2, $\beta=0$ for area of 1-cm radius in center, $\beta=0.8$ elsewhere). S_1 and S_2 were delivered at same site. P indicates that wave excited by S_2 propagates throughout tissue without reentry; F, that S_2 cannot stimulate a wave; F_R , that wave stimulated by S_2 can propagate but is blocked a distance away from pacing site; R, that S_2 induces reentry; and R_T , that S_2 induces transient reentry.

reduced (by setting $\beta=0.4$ in Equation 2), there was still a large vulnerable window for reentry (Figure 5E). In addition, a new phase was observed in which S_2 excited a propagating wave that was blocked a distance away from the pacing site.

If APD restitution was flattened (corresponding to Figure 1D), reentry could not be induced with the same degree of preexisting electrophysiological heterogeneity (Figure 5D). However, if the preexisting heterogeneity was increased to produce a steep local electrophysiological gradient, a small vulnerable window was observed (Figure 5F). In addition, a new phase occurred in which reentry was only transient.

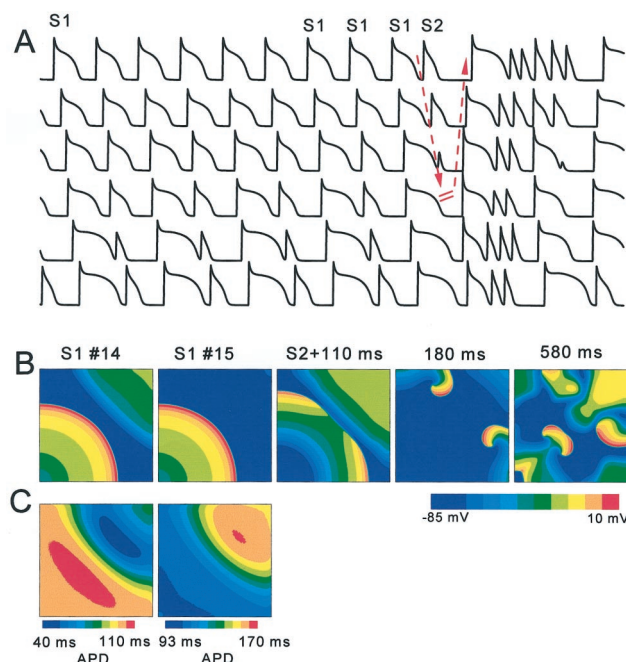


Figure 6. Induction of reentry in heterogeneous tissue with steep APD restitution plus normal CV restitution (as in Figure 1A). S_1 (15 beats at $PCL=170$ ms) and S_2 ($S_1S_2=120$ ms) were delivered at same site. A, Membrane potential at different sites in tissue, with conduction block initiating reentry indicated by arrows. B, Snapshots of membrane voltage during last 2 S_1 beats (beats 14 and 15) and at various times after S_2 was delivered, showing initiation of figure-eight reentry leading to fibrillation. C, Spatial APD distribution for S_1 beats 14 and 15, showing discordant alternans.

Thus, with sufficiently large electrophysiological heterogeneity, reentry could be induced even when APD restitution was flat enough to prevent discordant (or even concordant) alternans.

Mechanisms of Initiation of Reentry

It is generally argued that discordant alternans facilitates induction of reentry by increasing dispersion of refractoriness. However, a detailed mechanistic explanation is lacking. To this end, Figure 7A illustrates schematically 2 successive waves in the tissue. During wave propagation, both wavefront conduction velocity (CVF) and the waveback conduction velocity (CVB) vary in time and space. Conduction fails when the wavefront velocity is below a critical velocity CVF_c .²⁰ For local conduction block, eg, at location a in Figure 7A, CVB_1 must be slower than CVF_c at a, such that the wavefront of the second wave can approach closer and closer to the waveback of the first wave until CVF_2 becomes smaller than CVF_c . However, local wavebreak does not necessarily guarantee reentry. Wavebreak at point a may not lead to a reentry because the wavelength (and hence refractoriness) of the tissue in this region is long and the broken wave does not have sufficient surrounding excitable tissue nearby to execute a full turn. In contrast, wavebreak at point b is more likely to induce reentry, because the wavelength and refractory period are short. From this argument, it is easy to conceptualize the conditions favoring reentry: (1) a sufficiently slow propagating waveback to cause conduction failure; (2) inhomogene-

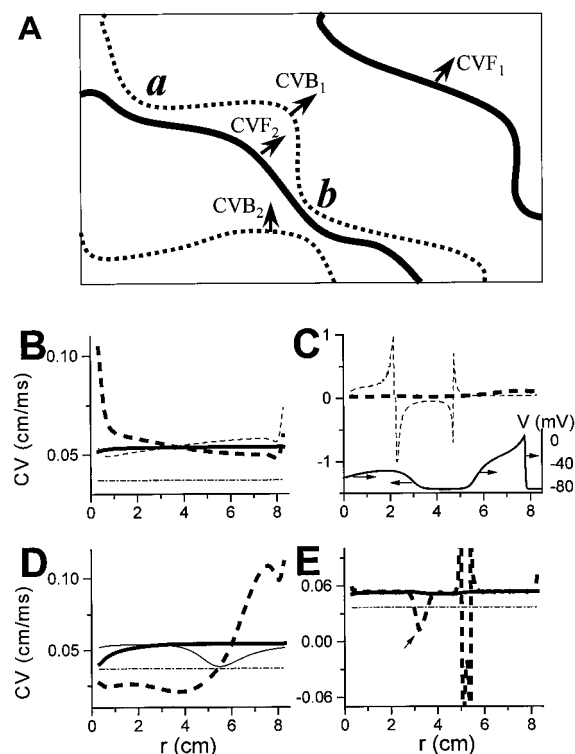


Figure 7. A, Schematic of successive waves in tissue, illustrating wavefront (thick lines) and waveback (thin lines) propagation (see text). B through E, Wavefront (solid lines) and waveback (dashed lines) velocities along tissue diagonal line (r) for 2 successive beats (thick and thin lines, respectively) in homogeneous tissue with steep APD restitution plus normal CV restitution (as in Figure 1A). Dashed-dotted lines indicate wavefront velocity at which conduction fails (CVF_c). B, Concordant alternans at $PCL=220$ ms. C and D, Discordant alternans at $PCL=180$ ms. C shows only waveback velocities, illustrating that 1 beat develops negative waveback velocity. Inset shows voltage in space, and arrows indicate propagation directions. D shows wavefront and waveback velocities of 1 beat (thick lines) and wavefront velocity of next beat (thin line). E, Wavefront and waveback velocities in markedly heterogeneous tissue with shallow APD restitution plus normal CV restitution described in Figure 5F. Arrow indicates that slow waveback occurs near boundary of heterogeneity.

ities to cause conduction failure locally; and (3) alternation of wavelength, or refractory period, to facilitate reentry.

With respect to slow propagation of a waveback, the relationship between CVB and CVF of a wave can be deduced as follows: the time for the waveback at position r to propagate a distance Δr is the time that the wavefront propagates this same distance $[\Delta r/CVF(r)]$ plus the APD difference between position $r+\Delta r$ and position r $[\Delta APD(r)=APD(r+\Delta r)-APD(r)]$, ie, $\Delta r/CVF(r)+\Delta APD(r)$. Therefore, the waveback velocity is given by the expression

$$(4) \quad CVB(r) = \frac{\Delta r}{\frac{\Delta r}{CVF(r)} + \Delta APD(r)} = \frac{CVF(r)}{1 + APD'(r) \cdot CVF(r)},$$

where $APD'(r) \approx \Delta APD(r)/\Delta r$ is the spatial derivative of APD. Equation 4 is similar to the equation derived by Courtemanche.²¹ From Equation 4, if the gradient

$APD'(r) > 0$, then $CVB(r) < CVF(r)$. If $APD'(r) < 0$ but $APD'(r) \cdot CVF(r) > -1$, then $CVB(r) > CVF(r)$. If $APD'(r) < 0$ but $APD'(r) \cdot CVF(r) < -1$, then $CVB(r) < 0 < CVF(r)$. Therefore, the back of a wave can propagate either slower or faster than its front, depending on the spatial gradient of APD. Two ways to produce large spatial APD gradients are discordant alternans and tissue heterogeneity.

Figure 7, B through D, shows CVF and CVB during pacing in homogeneous tissue with steep APD restitution plus normal CV restitution (corresponding to Figure 1A). At PCL=220 ms (Figure 7B), concordant alternans was present. Both CVF and CVB were almost the same except at the boundaries and were much larger than CVF_c . At PCL=180 ms (Figure 7, C and D), discordant alternans was present, and CVB varied greatly over space. In 1 of the 2 alternating beats, CVB changed from large positive to large negative velocity (Figure 7C). The negative velocity was due to the large decrease of APD along the direction of propagation (see Equation 4), which is illustrated in the inset at the bottom of Figure 7C. In a later beat (Figure 7D), the waveback propagated very slowly at first ($CVB \ll CVF$ and CVF_c) and then became faster than the wavefront. In contrast, Figure 7E shows CVF and CVB for heterogeneous tissue, with shallow APD restitution but steep gradient of electrophysiological heterogeneity in Figure 5F. A narrow area showing slow waveback propagation (much slower than CVF_c) is present at one boundary of the sharp heterogeneity, and CVB varies from positive to negative at the other boundary. The cause of the negative velocity is similar to that in Figure 7C.

Discussion

Our simulations show good agreement with the following experimental findings: (1) For a premature stimulus in heterogeneous tissue, there is an optimal coupling interval that minimizes dispersion of repolarization, after which dispersion increases.^{18,19} (2) During rapid pacing, there is a transition from constant APD to concordant alternans to discordant alternans. Concordant alternans is manifest electrocardiographically as T-wave alternans; discordant APD alternans is also associated with CL alternans, which causes QRS alternans in addition to T-wave alternans.⁹ (3) By markedly increasing dispersion of refractoriness, discordant alternans increases vulnerability to reentry.⁹ The close agreement with experimental observations supports the general validity of the model we used.

Our simulations provide some new insights into the cellular mechanisms of discordant alternans and how it leads to increased vulnerability to reentrant arrhythmias. By studying the roles of electrical restitution and preexisting electrophysiological heterogeneity, we reached the following conclusions.

Modulation of Dispersion by a Premature Stimulus

The mechanism by which a premature stimulus modulates dispersion agrees with the conjecture by Laurita et al¹⁸: a short S_1S_2 coupling interval results in a short DI for the premature beat. The premature beat thus propagates more slowly than the normal beats, so that DIs along the propagation direction increase, which, in turn, result in longer APD

(see Figure 2C). In homogeneous tissue, this results in a monotonic increase in dispersion as S_1S_2 decreases. However, in electrophysiologically heterogeneous tissue, both APD restitution and preexisting heterogeneity are important for modulation of dispersion. If APD restitution is steep, the long APD is markedly shortened by a short DI, whereas the shorter APD is only modestly shortened by a longer DI. This results in less dispersion (Figure 2B). CV restitution changes the coupling interval and thus changes the dispersion.

Mechanism of Concordant and Discordant APD Alternans

For APD alternans (concordant or discordant) to occur, an APD restitution slope >1 is required, even in electrophysiologically heterogeneous tissue. During pacing from the same site, to proceed from concordant to discordant alternans requires that the PCL be short enough to engage CV restitution. CV restitution explains why discordant alternans is associated with QRS as well as T-wave alternans. Neither concordant nor discordant alternans requires preexisting electrophysiological heterogeneity; they can arise solely from the dynamics of electrical restitution. (See the Appendix for formal analysis of the mechanism.) Although for large heterogeneous initial conditions, transient discordant alternans can be initiated without engaging CV restitution, alternans will finally become concordant.

Facilitation of Reentry

Discordant alternans markedly increases dispersion of refractoriness and increases the ability of a premature stimulus to cause localized wavebreak and induce reentry, even in completely homogeneous tissue. Preexisting electrophysiological heterogeneity is not required if the S_2 extrastimulus is delivered at a different site from the S_1 pacing site. In the absence of discordant alternans, preexisting electrophysiological heterogeneity can also cause localized wavebreak.

Although reentry can be induced with or without steep APD restitution, the vulnerability is different. When APD restitution is shallow, wavebreak occurs only in regions with very large preexisting heterogeneity. Because APD and wavelength are long, reentry cannot be easily induced (Figure 5), eg, at location a in Figure 7A. The vulnerable window of reentry is much larger when APD restitution is steep enough to produce discordant alternans (Figure 5), because during discordant alternans, wavebreak always occurs in the waves with short APD and wavelength (eg, at location b in Figure 7A).

In summary, heterogeneity breaks symmetry and also can cause wavebreak by waveback slowing; APD restitution causes the dynamical instability, resulting in wavelength oscillation; CV restitution converts concordant APD alternans into discordant alternans, which results in further waveback slowing and increased dispersion of refractoriness.

Clinical Implications

Combined with experimental evidence relating discordant APD alternans to T-wave alternans and increased vulnerability to ventricular arrhythmias,¹⁻¹⁰ our findings further emphasize the importance of dispersion of refractoriness to induction of ventricular reentry. Most importantly, our analysis suggests that dispersion of refractoriness arising from purely dynamic factors, namely APD and CV restitution, is at least as

important as, if not more important than, preexisting electrophysiological heterogeneity for enhancing susceptibility to ventricular arrhythmias. This is therapeutically encouraging, because restitution properties are potentially modifiable by drugs. Drugs altering electrical restitution to reduce dynamic dispersion represent a promising antiarrhythmic strategy.

Appendix

Mechanism of Discordant Alternans

Assume APD and CV restitution are valid in a spatially uniform system:

$$(5) \quad \text{APD}_{n+1}(r) = f[DI_n(r)] = F[CL_n(r) - \text{APD}_n(r)], \\ \text{CV}_{n+1}(r) = g[DI_n(r)].$$

In Equation 5, $CL_n(r)$ can be expressed as

$$(6) \quad \begin{aligned} CL_n(r) &= PCL + \int_0^r \frac{dr'}{CV_{n+1}(r')} - \int_0^r \frac{dr'}{CV_n(r')} \\ &= PCL + \int_0^r \frac{CV_n(r') - CV_{n+1}(r')}{CV_{n+1}(r') \cdot CV_n(r')} dr' \\ &= PCL + \int_0^r \frac{-\Delta CV(r')}{CV_{n+1}(r') \cdot CV_n(r')} dr' \\ &= PCL + \Delta CL_n(r) \\ &= \text{APD}_n(r) + DI_n(r). \end{aligned}$$

Starting from a uniform initial condition, we can derive from Equations 5 and 6 the following.

1. For long PCLs without APD alternans, the system remains uniform.
2. For PCLs at which APD alternates but CV restitution is not engaged, $CV_{n+1}(r) = CV_n(r)$. In this case, the integral in Equation 6 is zero, ie, $\Delta CL_n(r) = 0$. Therefore, $CL_n(r) = PCL$ everywhere in space, which indicates from Equation 5 that $\text{APD}_n(r)$ and $DI_n(r)$ must both be uniform in space, ie, uniform concordant alternans occurs.
3. For PCLs in a range in which both APD alternans occurs and CV restitution is engaged, assume that the system is in a stable alternating state such that $DI_{n+2}(r) = DI_n(r) > DI_{n-1}(r) = DI_{n+1}(r)$ at position r . According to Equation 6, $\Delta CL_n(r) = -\Delta CL_{n+1}(r)$ and $DI_n(r) = CL_n(r) - \text{APD}_n(r)$; we then have

$$(7) \quad \begin{aligned} DI_{n+1}(r) &= PCL - \Delta CL_n(r) - \text{APD}_{n+1}(r) < DI_n(r) = PCL \\ &\quad + \Delta CL_n(r) - \text{APD}_n(r). \end{aligned}$$

Rearranging and substituting Equation 7,

$$(8) \quad \begin{aligned} \text{APD}_{n+1}(r) - \text{APD}_n(r) &> -2\Delta CL_n(r) \\ &= 2 \int_0^r \frac{CV_{n+1}(r') - CV_n(r')}{CV_{n+1}(r') \cdot CV_n(r')} dr' > 0. \end{aligned}$$

Uniform concordant alternans, with $\text{APD}_{n+1}(r) - \text{APD}_n(r)$ constant over space, is impossible, because the integral in Equation 8 changes

with r . Nonuniform concordant alternans can exist when $CV_{n+1}(r) - CV_n(r)$ or r is small, for which Equation 8 can be satisfied. However, when either $CV_{n+1}(r) - CV_n(r)$ or r is large, then the integration in Equation 8 becomes larger and larger, and Equation 8 cannot hold for concordant alternans. Therefore, $CV_{n+1}(r) - CV_n(r)$ must change its sign along r so as not to violate Equation 8, resulting in discordant alternans.

Acknowledgments

This study was supported by NIH SCOR in Sudden Cardiac Death P50HL-52319, AHA Western States Affiliate Beginning Grant-in-Aid (to Dr. Qu), and the Laubisch and Kawata Endowments (Dr. Weiss).

References

1. Nearing BD, Huang AH, Verrier RL. Dynamic tracking of cardiac vulnerability by complex demodulation of the T wave. *Science*. 1991;252:437–440.
2. Rosenbaum DS, Jackson LE, Smith JM, et al. Electrical alternans and vulnerability to ventricular arrhythmias. *N Engl J Med*. 1994;330:235–241.
3. Verrier RL, Nearing BD. Electrophysiologic basis for T wave alternans as an index of vulnerability to ventricular fibrillation. *J Cardiovasc Electrophysiol*. 1994;5:445–461.
4. Armondas AA, Osaka M, Mela T, et al. T-wave alternans and dispersion of the QT interval as risk stratification markers in patients susceptible to sustained ventricular arrhythmias. *Am J Cardiol*. 1998;82:1127–1129, A9.
5. Euler DE. Cardiac alternans: mechanisms and pathophysiological significance. *Cardiovasc Res*. 1999;42:583–590.
6. Konta T, Ikeda K, Yamaki M, et al. Significance of discordant ST alternans in ventricular fibrillation. *Circulation*. 1990;82:2185–2189.
7. Rubenstein DS, Lipsius SL. Premature beats elicit a phase reversal of mechano-electrical alternans in cat ventricular myocytes: a possible mechanism for reentrant arrhythmias. *Circulation*. 1995;91:201–214.
8. Tachibana H, Kubota I, Yamaki M, et al. Discordant S-T alternans contributes to formation of reentry: a possible mechanism of reperfusion arrhythmia. *Am J Physiol*. 1998;275:H116–H121.
9. Pastore JM, Girouard SD, Laurita KR, et al. Mechanism linking T-wave alternans to the genesis of cardiac fibrillation. *Circulation*. 1999;99:1385–1394.
10. Cao JM, Qu Z, Kim YH, et al. Spatiotemporal heterogeneity in the induction of ventricular fibrillation by rapid pacing: importance of cardiac restitution properties. *Circ Res*. 1999;84:1318–1331.
11. Nolasco JB, Dahlen RW. A graphic method for the study of alternation in cardiac action potentials. *J Appl Physiol*. 1968;25:191–196.
12. Vinet A, Chialvo DR, Michaels DC, et al. Nonlinear dynamics of rate-dependent activation in models of single cardiac cells. *Circ Res*. 1990; 67:1510–1524.
13. Courtemanche M, Glass L, Keener JP. Instabilities of a propagating pulse in a ring of excitable media. *Phys Rev Lett*. 1993;70:2182–2185.
14. Koller ML, Riccio ML, Gilmour RF Jr. Dynamic restitution of action potential duration during electrical alternans and ventricular fibrillation. *Am J Physiol*. 1998;275:H1635–H1642.
15. Qu Z, Weiss JN, Garfinkel A. Cardiac electrical restitution properties and the stability of reentrant spiral waves: a simulation study. *Am J Physiol*. 1999;276:H269–H283.
16. Luo CH, Rudy Y. A model of the ventricular cardiac action potential: depolarization, repolarization, and their interaction. *Circ Res*. 1991;68: 1501–1526.
17. Qu Z, Garfinkel A. An advanced numerical algorithm for solving partial differential equation in cardiac conduction. *IEEE Trans Biomed Eng*. 1999;49:1166–1168.
18. Laurita KR, Girouard SD, Rosenbaum DS. Modulation of ventricular repolarization by a premature stimulus: role of epicardial dispersion of repolarization kinetics demonstrated by optical mapping of the intact guinea pig heart. *Circ Res*. 1996;79:493–503.
19. Laurita KR, Girouard SD, Akar FG, et al. Modulated dispersion explains changes in arrhythmia vulnerability during premature stimulation of the heart. *Circulation*. 1998;98:2774–2780.
20. Zykov VS. *Simulation of Wave Process in Excitable Media*. New York, NY: Manchester University Press; 1982.
21. Courtemanche M. Complex spiral wave dynamics in a spatially distributed ionic model of cardiac electrical activity. *Chaos*. 1996;6:579–600.

Mechanisms of Discordant Alternans and Induction of Reentry in Simulated Cardiac Tissue

Zhilin Qu, Alan Garfinkel, Peng-Sheng Chen and James N. Weiss

Circulation. 2000;102:1664-1670

doi: 10.1161/01.CIR.102.14.1664

Circulation is published by the American Heart Association, 7272 Greenville Avenue, Dallas, TX 75231

Copyright © 2000 American Heart Association, Inc. All rights reserved.

Print ISSN: 0009-7322. Online ISSN: 1524-4539

The online version of this article, along with updated information and services, is located on the World Wide Web at:

<http://circ.ahajournals.org/content/102/14/1664>

Permissions: Requests for permissions to reproduce figures, tables, or portions of articles originally published in *Circulation* can be obtained via RightsLink, a service of the Copyright Clearance Center, not the Editorial Office. Once the online version of the published article for which permission is being requested is located, click Request Permissions in the middle column of the Web page under Services. Further information about this process is available in the [Permissions and Rights Question and Answer](#) document.

Reprints: Information about reprints can be found online at:
<http://www.lww.com/reprints>

Subscriptions: Information about subscribing to *Circulation* is online at:
<http://circ.ahajournals.org/subscriptions/>